

STRUCTURE, PROPERTIES, AND PROCESSING OF TWO-PHASE CRYSTALLINE-AMORPHOUS  
W-BASED ALLOYS

T. H. COURTNEY

AUGUST, 2000

U. S. ARMY RESEARCH OFFICE

GRANT NO. DAAG55-98-1-0082

MICHIGAN TECHNOLOGICAL UNIVERSITY

APPROVED FOR PUBLIC RELEASE:  
DISTRIBUTION UNLIMITED

THE VIEWS, OPINIONS, AND/OR FINDINGS CONTAINED IN THIS REPORT ARE THOSE OF  
THE AUTHOR AND SHOULD NOT BE CONSIDERED AS AN OFFICIAL DEPARTMENT OF THE  
ARMY POSITION, POLICY, OR DECISION, UNLESS SO DESIGNATED BY OTHER  
DOCUMENTATION.

## REPORT DOCUMENTATION PAGE

Form Approved  
OMB NO. 0704-0188

Public reporting burden for this collection of information is estimated to average 1 hour per response, including the time for reviewing instructions, searching existing data sources, gathering and maintaining the data needed, and completing and reviewing the collection of information. Send comment regarding this burden estimate or any other aspect of this collection of information, including suggestions for reducing this burden, to Washington Headquarters Services, Directorate for Information Operations and Reports, 1215 Jefferson Davis Highway, Suite 1204, Arlington, VA 22202-4302, and to the Office of Management and Budget, Paperwork Reduction Project (0704-0188), Washington, DC 20503.

1. AGENCY USE ONLY (Leave blank)	2 REPORT DATE	3 REPORT TYPE AND DATES COVERED	
	August 2000	Final: February 1998 - August 2000	
4 TITLE AND SUBTITLE  Structure, Properties, and Processing of Two-Phase Crystalline-Amorphous W-Based Alloys			5 FUNDING NUMBERS  DAAG55-98-1-0082
6. AUTHOR(S)  T. H. Courtney			
7. PERFORMING ORGANIZATION NAMES(S) AND ADDRESS(ES)  Department of Materials Science and Engineering Michigan Technological University 1400 Townsend Drive Houghton, MI 49931			8. PERFORMING ORGANIZATION REPORT NUMBER
9. SPONSORING / MONITORING AGENCY NAME(S) AND ADDRESS(ES)  U.S. Army Research Office P.O. Box 12211 Research Triangle Park, NC 27709-2211			10. SPONSORING / MONITORING AGENCY REPORT NUMBER  ARO 37567.3-ms
11. SUPPLEMENTARY NOTES  The views, opinions and/or findings contained in this report are those of the author(s) and should not be construed as an official Department of the Army position, policy or decision, unless so designated by other documentation.			
12a. DISTRIBUTION / AVAILABILITY STATEMENT  Approved for public release; distribution unlimited.		12 b. DISTRIBUTION CODE	
13. ABSTRACT (Maximum 200 words)  The thermal stability and crystallization behavior of noncrystalline W-Ni alloys have been investigated. These materials are generated by the mechanical alloying process. The powders so produced consist of a noncrystalline matrix containing a dispersion of nanometer-sized crystalline W particles. We find that the crystallization temperatures of these materials are tied closely to the W content in the amorphous phase. This composition can be varied by alterations in either the overall W content of the alloy or the mechanical alloying time. Thermal stability studies - monitored by differential scanning calorimetry, x-ray diffraction, and transmission electron microscopy - have identified promising thermally stable noncrystalline W compositions. Consolidation of mechanically alloyed noncrystalline powders absent their crystallization is difficult. Several promising consolidation routes have been identified. These may permit production of fully dense noncrystalline powders in bulk form. Such material may have potential as kinetic energy penetrators.			
14. SUBJECT TERMS  Mechanical alloying, tungsten heavy alloys, noncrystalline tungsten alloys, powder processing			15. NUMBER OF PAGES  17
			16. PRICE CODE
17. SECURITY CLASSIFICATION OR REPORT  UNCLASSIFIED	18. SECURITY CLASSIFICATION OF THIS PAGE  UNCLASSIFIED	19. SECURITY CLASSIFICATION OF ABSTRACT  UNCLASSIFIED	20. LIMITATION OF ABSTRACT  UL

## Table of Contents

	Page
I. Introduction and Overview	1
II. Crystallization and Thermal Stability of W-Ni-Fe Glassy Metals	1
A. Background	1
B. Experimental Procedure	2
C. Results and Discussion	4
i – Milled Powders	4
ii – Thermal Stability of 50 at. % W Alloys	4
iii – Thermal Stability of 75 at. % W Alloys	7
iv - Summary	11
III. Consolidation Studies	11
A. Hot Isostatic Pressing (HIP)	11
B. Dynamic Compaction	13
C. Hot Isostatic Pressing with a "Binding Agent"	13
IV. Future Work	14
A. Thermodynamics of the Ni-W System	14
B. Consolidation Studies	15
V. List of Publications	15
VI. Scientific Personnel Supported	16
VII. References	17

List of Illustrations and Tables

Page No.	Table/Figure	Title
3	Table 1	Fe content in the as-milled powder
3	Figure 1	(a) X-ray diffraction patterns for 50 at. % W powders milled for different times. Volume fraction of crystalline W and the estimated W atomic fraction in the noncrystalline phase as a function of milling time for (b) the 50 at. % W alloy and (c) the 75 at. % W alloy.
5	Figure 2	DSC trace (10 K/min) for the 50 at. % W sample milled for 40 hr. The arrows indicate the apparent crystallization reactions and their associated temperatures.
5	Figure 3	X-ray diffraction patterns illustrating phase evolution in the 50 at. % W alloy powders milled for 40 hr and heated to various temperatures.
6	Figure 4	Crystalline W volume fraction evolution at different temperatures for 50 at. % W alloy milled for 40 hr. The vertical lines indicate the onset temperature of each reaction.
6	Figure 5	TEM diffraction pattern of the 50 at. % W alloy milled for 40 hr and then heated to 620° C. The broad diffuse ring is indicative of a noncrystalline phase.
8	Figure 6	TEM diffraction pattern of the 50 at. % W alloy milled for 40 hr and then heated to 680° C. In addition to crystalline diffraction spots, a diffuse ring – indicative of a noncrystalline phase – is observed.
8	Figure 7	Backscattered scanning-electron micrograph of a 50 at. % W alloy milled for 40 hr and then heated to 850° C. Tungsten is light, NiW gray, and the Ni-rich phase is black. The microstructural scale is on the order of 0.1 μm.
9	Figure 8	DSC traces for the 75 at. % W alloys milled for (a) 10 hr, (b) 20 hr. The arrows indicate the crystallization reaction(s) and their associated temperatures.

- 9       Figure 9      Crystalline W volume fraction at different temperatures for 75 at. % W alloy milled for 10 hr. The vertical lines indicate the onset temperature for each reaction. A three- stage crystallization sequence, similar to that found for the 50 at. % W alloy, is followed.
- 10      Figure 10     Crystalline W volume fraction at different temperature for 75 at. % W alloy milled for 20 hr.
- 10      Figure 11     First reaction peak temperature vs. W contents in the glassy phase in the as-milled powders. (Times shown are milling times.) The reaction temperature appears to be directly related to the initial glassy-phase W content.
- 12      Figure 12     Peak temperatures for the high-temperature crystallization reaction vs. W content (a) in the glassy phase in the as-milled powders, and (b) in the glassy phase present prior to the high-temperature reaction. (The times shown are milling times.)

## I. Introduction and Overview

This program has a technological objective, viz. to develop fully dense W heavy alloys (WHA) consisting of a glassy matrix in which nanometer-sized W particles are imbedded. These materials might be more suitable than conventional WHA for use as kinetic energy penetrators (perhaps armor, too). Conventional WHA penetrators are prone to tip blunting which negatively impacts performance. Glassy metals, on the other hand, flow by shear band formation and propagation. In tension, only one of these localized "packets" of plasticity forms prior to material fracture. However, in certain metallic glasses a suitable dispersion of fine particles can induce multiple shear banding in tension [1-5]. Our previous ARO sponsored work has suggested the multiple shear banding is a result of deformation constraints placed on the glassy matrix by a bonding metal [6-8]. If WHA can be made having such structures it is possible that they will manifest multiple shear banding during penetration. Then, in analogy with depleted uranium (DU), such a modified WHA penetrator will maintain its tip profile during penetration. The difference between the modified WHA and DU is that multiple shear banding in DU is induced by adiabatic plastic deformation and/or an allotropic transformation induced by tip heating during penetration whereas multiple shear banding in the glassy WHA would be intrinsic in nature.

The technical challenges to produce such WHA are daunting. There is no problem in producing glassy WHA powders containing nanometer-sized crystalline W particles. We first did this about ten years ago, employing mechanical alloying (MA) processing [9]. However, powder consolidation is not easy. In particular, consolidation can only take place between the glassy metal's glass transition ( $T_g$ ) and crystallization ( $T_x$ ) temperatures. The WHA glassy metals are not intrinsically strong glass formers. That is, the temperature difference between  $T_g$  and  $T_x$  is small, resulting in a narrow working temperature range for consolidation absent crystallization.

While there is a technological focus to our work, attainment of our goal requires basic studies. In our case, as is described later, we have conducted a systematic study of the effect of milling time and W content on the crystallization proclivities of WHA prepared by MA. This enables us to define processing routes that may permit maintenance of the desirable glassy phase microstructure during consolidation. In addition, we have pursued some "novel" consolidation techniques other than conventional hot isostatic pressing (HIP - this has been our usual consolidation procedure).

Three sections follow. First, results of processing and glass-phase stability studies are described. These are at an advanced stage. (A recently submitted [10] paper details these.) Then we present the results of consolidation studies; they have not yet been as fruitful. Finally, we describe plans for the forthcoming year.

## II. Crystallization and Thermal Stability of W-Ni-Fe Glassy Metals

### A. Background

A few comments on the development of noncrystalline structures in mechanically alloyed Ni-W alloys are in order; details can be found in [9]. During MA of elemental mixtures of Ni and W, W dissolves in the Ni-rich phase. If the W content is less than about 28 at. %, a supersaturated solid solution develops after sufficiently long milling times. However, if the W content exceeds ca. 28 at. %, the fcc phase amorphizes when the W content in it exceeds this value. With further increases in overall alloy W content, remnant W is present as nanometer-sized crystals in the glassy matrix. Initial W contents of the W-Ni alloys discussed here range from 50 to 75 at. %. Thus, our mechanically alloyed materials have a glassy matrix containing nanocrystalline W particles. The amount of this W is a function of alloy composition and MA time.

### B. Experimental Procedure

Details relative to processing and structural analysis are given in [10]. Here only the most pertinent procedures are described. Elemental Ni and W powders (-325 mesh, purity > 99%) were starting materials. The two initial compositions noted above were investigated.<sup>1</sup> These were mechanically alloyed in a SPEX mill for various times. Previous work in our laboratory has shown that the 50 at. % W alloys could be amorphized by milling for 10 hr. Thus, the 50 at. % W alloys were milled for times between 10 and 40 hr. Amorphization occurs more rapidly for alloys having a higher initial W content. For 75 at. % W samples, 5 hr of milling results in powder amorphization; therefore, 75 at. % W samples were milled for times between 5 and 20 hr.

Due to mill abrasion, Fe contamination of the powders occurs [11]. The extent of this was assessed by X-ray fluorescence spectroscopy and/or by measurement of the mass loss of the milling vial and grinding balls during milling. Iron contents so derived are given in Table 1. It has been reported that Fe does not significantly affect the solution and amorphization kinetics during MA of Ni-W powders [10]. Furthermore, Fe and Ni chemically behave similarly in these alloys. For example, Fe is found only in the amorphous phase and not in crystalline W during amorphization[10]. And on crystallization of the amorphous powders, Fe and Ni are present in proportion to their overall composition in the resulting fcc and intermetallic phases [12]. Even though the Fe contamination reduces the W content in the alloys, for convenience we refer to the alloys as 50 at. % W and 75 at. % W alloys throughout this report.

Following milling, the powders were examined by X-ray diffraction (XRD; Cu K $\alpha$  radiation). The Ni-W solid solution was taken as fully amorphous when the crystallite size estimated using the Scherrer line-broadening formula was less than 5 nm. Diffraction patterns corresponding to this situation are shown later.

Crystallization was monitored via differential scanning calorimetry (DSC) at various heating rates to a maximum temperature of 850° C. In addition to continuous heating to this temperature, other samples were heated to intermediate temperatures. After cooling, these were examined by XRD. The volume fraction of crystalline W in the powders was also measured by XRD using a variation of the internal standard method

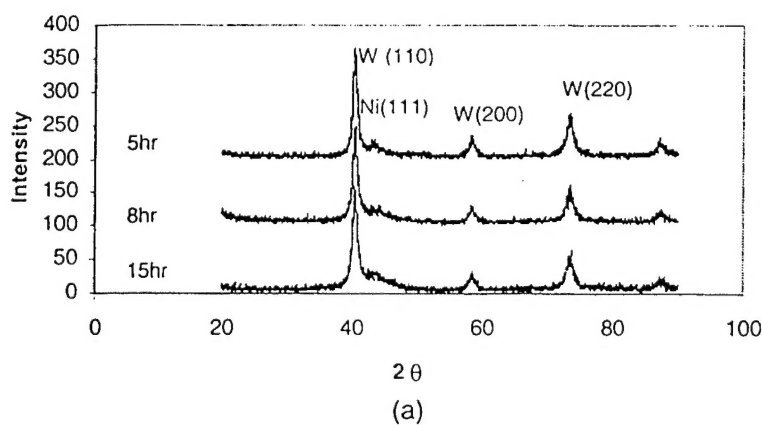
---

<sup>1</sup> - We are currently investigating 60 at. % W alloys. However, analysis of these alloys is not yet complete.

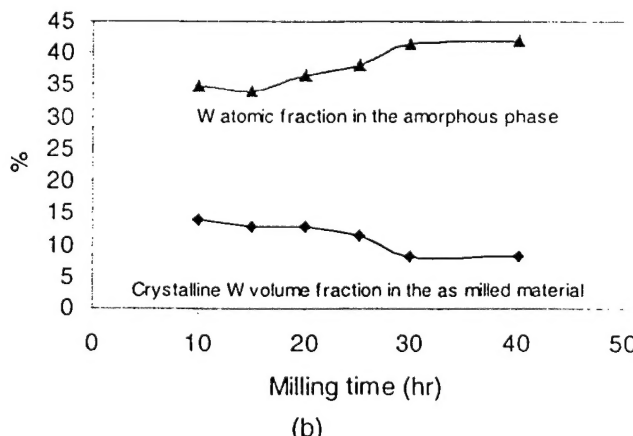
Table 1. Fe content in the as-milled powder\*

50 at. %W samples		75 at. %W-Ni samples	
Milling time (hrs)	Fe content (at. %)	Milling time (hrs)	Fe content (at. %)
10	7.9	5	7
15	8.5 (*), 10.6	6	11
20	8.3 (*)	7	13
25	8.2 (*), 7.9	8	13
30	14.7	10	18.3
40	12.8	15	20.7
		20	19.5

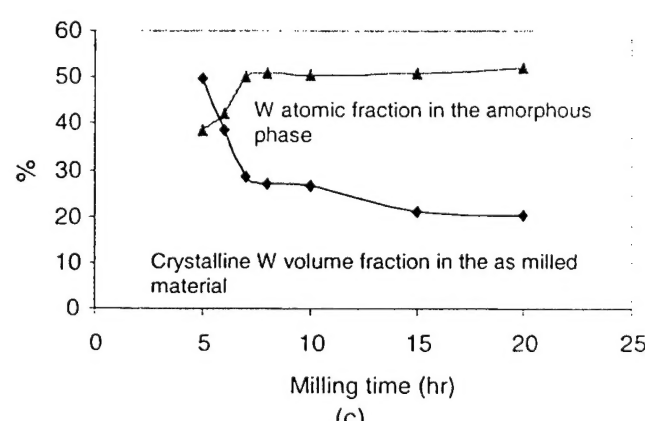
\*- Obtained by XRF except for compositions with (\*), they were estimated by measuring the mass loss of the vial and grinding media following milling.



(a)



(b)



(c)

Fig.1. (a) X-ray diffraction patterns for 50 at. % W powder milled for different times. Volume fraction of crystalline W and the estimated W atomic fraction in the noncrystalline phase as a function of milling time for (b) the 50 at. % W alloy and (c) the 75 at. % W alloy.

[13]. Microstructure was examined by backscattered electron microscopy (SEM). Transmission electron microscopy (TEM) was also selectively employed.

### C. Results and Discussion

#### i - Milled Powders

Previous work has shown that W dissolves in the Ni-rich fcc phase during MA [9]. This increases its lattice parameter, and the Ni {111} peak shifts to a lower diffraction angle. Following amorphization of the fcc phase, the XRD pattern shows a broad amorphous peak along with diffraction peaks of residual crystalline W (e.g., Fig. 1a). No diffraction peak of Fe can be identified in the XRD patterns and the solubility of Fe in crystalline W is limited. Thus, Fe can be considered present only in the Ni-rich phase(s). The microstructure of the milled powder is characterized by nanocrystalline W particles (ca. 15-20 nm in diameter) embedded in a W-Ni-Fe glassy matrix.

Volume fractions of the residual crystalline W are shown in Figs. 1b and 1c for the two alloys as a function of milling time. As anticipated, the amount of residual W decreases with milling time. Knowing the amount of this W, a mass balance yields the W content in the amorphous phase, as is also shown in Figs. 1b and 1c.

#### ii - Thermal Stability of 50 at. % W Alloys

The thermal stability and phase evolution during heating 50 at. % W-Ni as-milled powders were examined using DSC and XRD. A DSC trace for the sample milled for 40 hr is shown in Fig. 2. Three exothermic peaks, suggesting three reactions, are found.

Detailed analysis was conducted on the 50 at. % W alloys milled for 40 hr. The XRD patterns of these powders heated to different temperatures (heating rate = 10 K/min) are shown in Fig. 3. At 570° C, the onset temperature for the first reaction, the diffraction pattern is identical to that of the as-milled powder; bcc W peaks and a diffuse amorphous "peak" are found. However, the W volume fraction increases with increasing exposure temperature. For example, as shown in Fig. 4, this fraction increases from about 10 vol. % (characteristic of the milled powder) at 570° C to about 30% at 620° C (a temperature between the first- and second reaction peak temperatures indicated by DSC).

The XRD pattern of Fig. 3 indicates two phases – bcc W and a glassy phase – remain after the first reaction. The increase in the amount of W in the first reaction indicates that it precipitates from the glass during it. A mass balance permits estimation of the glassy-phase W content as 31 at. % following the first reaction. (This composition is still greater than both the equilibrium solubility (about 13 at. % [14]) and the critical composition (ca. 28 at. %) required for amorphization.) Fig. 5 is a TEM diffraction pattern of the material heated to 620° C. The pattern also shows the presence of an amorphous phase.

The onset temperature of the second reaction is about 650° C. The XRD pattern of Fig. 3 shows that for a sample heated to 680° C, an fcc {111} peak is present in addition to

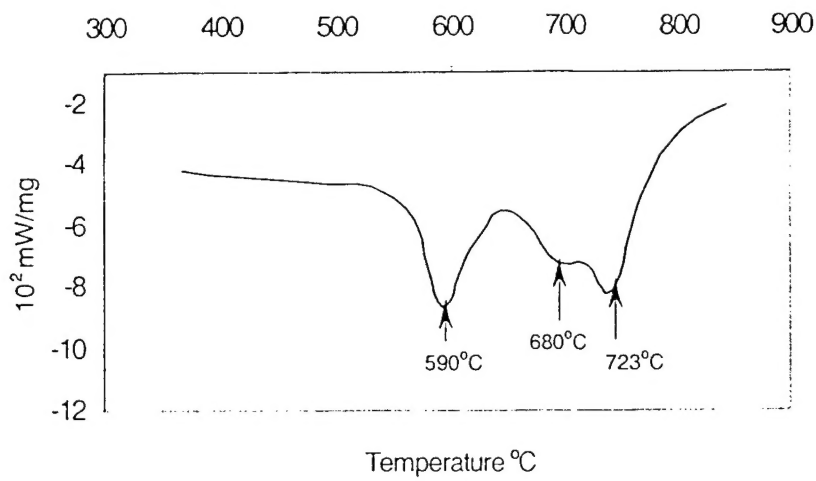


Fig. 2 DSC trace (10 K/min.) for the 50 at. %W sample milled for 40 hr. The arrows indicate the apparent crystallization reactions and their associated temperatures.

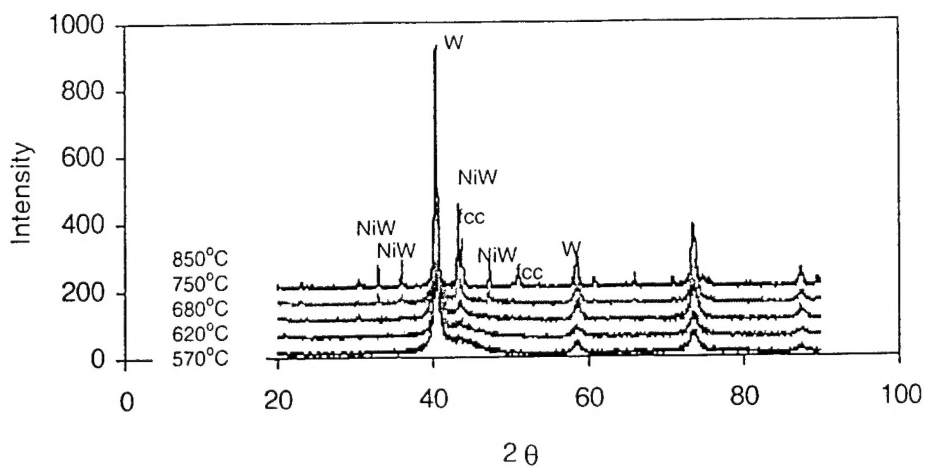


Fig.3 X-ray diffraction patterns illustrating phase evolution in the 50 at. % W alloy powders milled for 40 hr and heated to various temperatures.

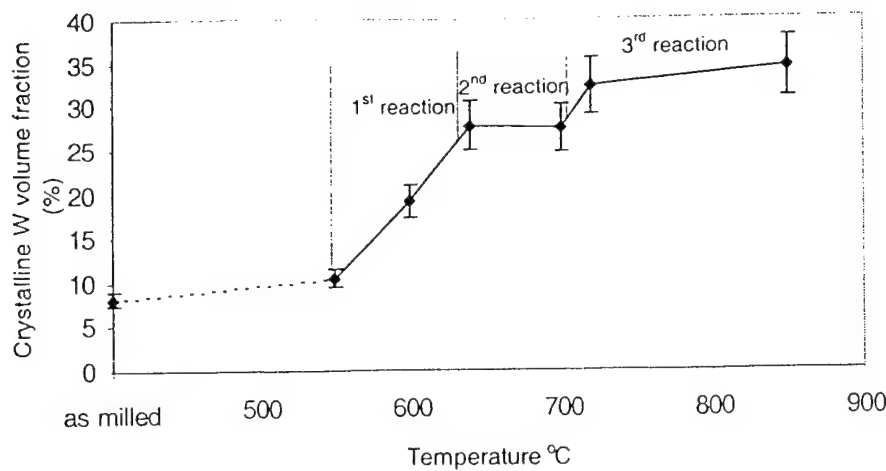


Fig.4 Crystalline W volume fraction evolution at different temperature for 50 at. % W alloy milled for 40 hr. The vertical lines indicate the onset temperature of each reaction.

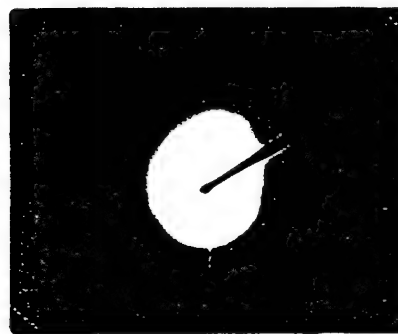


Fig.5 TEM diffraction pattern of the 50 at. %W alloy milled for 40 hr and then heated to 620°C. The broad diffuse ring is indicative of a noncrystalline phase.

W peaks. Thus crystallization of some of the glassy phase takes place during the second reaction. The W content of the fcc phase (about 19 at. % based on its lattice parameter) is not greatly in excess of the equilibrium solubility. However, Fig. 4 indicates that the W volume fraction hardly changed as a result of the second reaction, and it should increase if all of the glassy phase had transformed to a fcc phase having a W content of 19 at. %. On this basis, it appears that only partial crystallization of the glassy phase takes place during the second reaction. The TEM diffraction pattern of Fig. 6, indicating the presence of both a glassy and a crystalline phase, supports this view.

Following the third reaction, two intermetallics (NiW and Ni<sub>4</sub>W) are present in addition to W and the fcc phase. From the XRD pattern of Fig. 3, NiW can be clearly identified, but the presence of Ni<sub>4</sub>W is not obvious. This could be a result of the amount of this phase being small or because the strongest peaks of it superimpose on those of the fcc phase [15]. However, the presence of Ni<sub>4</sub>W has been confirmed by TEM [10].

The amount of crystalline W also increases in the third reaction (Fig. 4). This might be due to precipitation of W from the supersaturated fcc phase (a product of the second reaction) or during the crystallization of the noncrystalline phase remaining subsequent to the second reaction. The SEM micrograph of Fig. 7 illustrates the phase morphology in powders heated to 850° C. Three phases – W (white), NiW (gray), and the fcc phase (black) - are evident. The microstructural scale of the crystalline material is fine, on the order of 0.1 μm.

### iii - Thermal Stability of 75 at. % W Alloys

X-ray diffraction of the 75 at. % W alloys shows that their final crystallization products are the same as in the 50 at. % W alloys. However, DSC indicates that the crystallization process of the 75 at. % W alloys depends on the MA time. Specifically, two different crystallization scenarios are observed depending on this time (Fig. 8). For the powders milled for 10 hr, the three-stage crystallization process described previously occurs. But for the sample milled for 20 hr, only one exothermic peak is evident in the DSC curve. The “transition” milling time for the different situations is about 15 hr. Two samples (milled for 10 and 20 hr, respectively) representing the different crystallization behavior are compared and analyzed here.

X-ray diffraction patterns for the 75 at. % W powders milled for 10 hr and heated to various temperatures parallel those of the 50 at. % W alloys (cf., Fig. 3). Likewise, as shown in Fig. 8, three exothermic peaks are observed for this material. Although the first broad low-temperature exotherm for the 75 at. % W alloy milled for 10 hr is not striking, the amount of crystalline W increases from about 30 to 45 vol. % as the temperature is increased to 650° C (Fig. 9). Figure 9 also shows that the volume fraction of W increases (from 45 to 55 vol. %) in the third reaction. However, this fraction does not change much during the second reaction. These observations suggest that this material crystallizes in rather much the same manner as the 50 at. % W alloys.

For the 75 at. % W alloys milled for times in excess of 15 hr, DSC detects only one reaction on heating to 850° C (Fig. 8b). XRD shows that crystallization does not occur

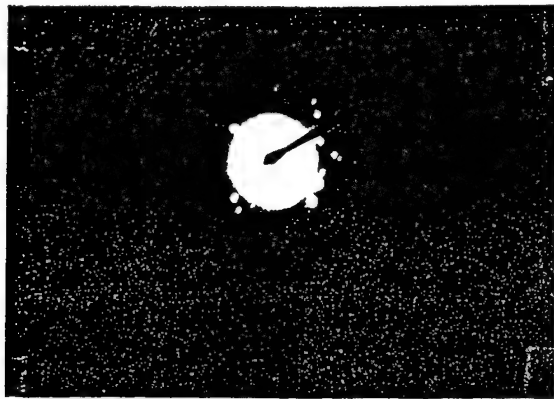


Fig.6 TEM diffraction pattern of the 50 at. % W alloy milled for 40hr and then heated to 680°C. In addition to crystalline diffraction spots, a diffuse ring – indicative of a noncrystalline phase – is observed.

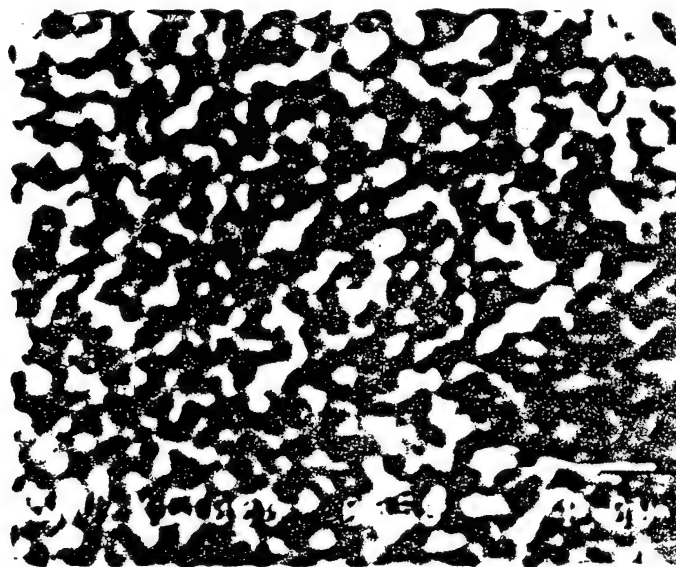
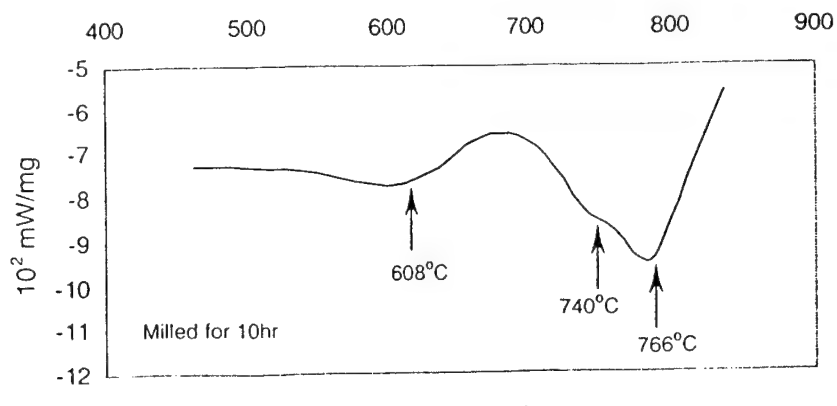
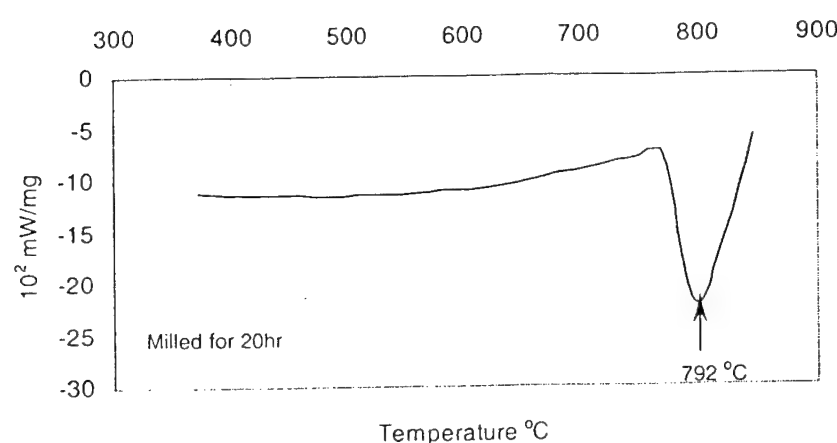


Fig. 7. Backscattered scanning-electron micrograph of 50 at. % W alloy milled for 40 hr and heated to 850° C. Tungsten is light, NiW gray, and the Ni-rich phase is black. The microstructural scale is on the order of 0.1  $\mu$ m.



(a)



(b)

**Fig. 8.** DSC traces for the 75 at. % W alloys milled for (a) 10 hr, (b) 20 hr. The arrows indicate the crystallization reaction(s) and their associated temperatures.

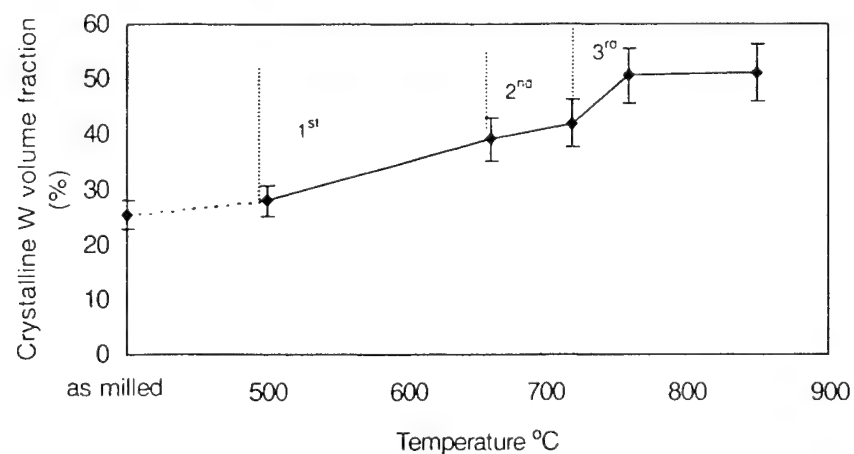


**Fig. 9.** Crystalline W volume fraction at different temperatures for 75 at. % W alloy milled for 10 hr. The vertical lines indicate the onset temperature for each reaction. A three-stage crystallization sequence, similar to that found for the 50 at. % W alloys, is followed.

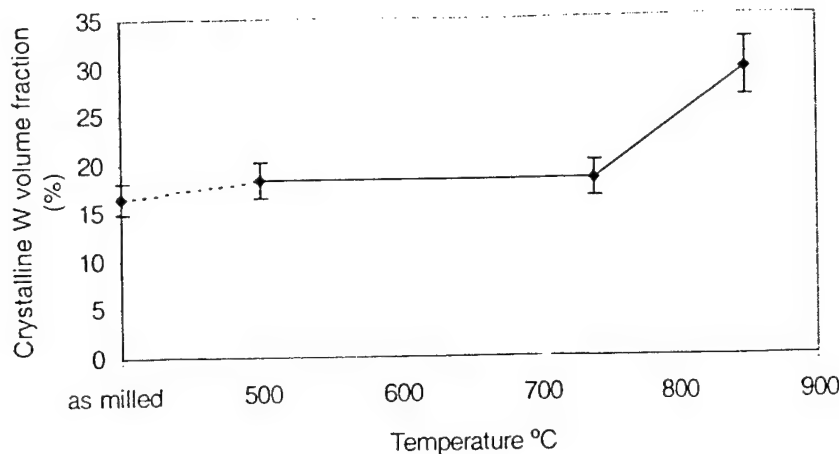


Fig. 10. Crystalline W volume fraction at different temperatures for 75 at. % W alloy milled for 20 hr.

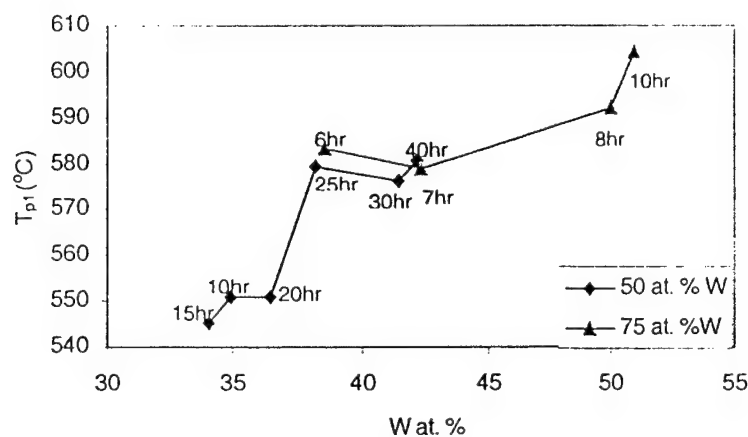


Fig. 11. First reaction peak temperatures vs. W contents in the glassy phase in the as-milled powders. (Times shown are milling times.) The reaction temperature appears to be directly related to the initial glassy-phase W content.

until the temperature exceeds 750° C. Figure 10 also verifies that the W volume fraction does not increase until this temperature is exceeded.

Figure 11 plots the first reaction peak temperature as it varies with the glassy-phase W composition. This temperature increases significantly with this W content (and with milling time) for both alloy compositions studied. It is noteworthy that the first peak temperature correlates primarily with the glassy-phase composition; i.e., this temperature increases monotonically with this composition and is apparently not significantly impacted per se by the overall W alloy content. The peak temperatures of the final crystallization stage are shown in Figs. 12.<sup>2</sup> The abscissa of Fig. 12a is the as-milled glassy-phase W content. When the third reaction temperatures are plotted vs. this composition, the temperatures more-or-less fall into two groups depending on the overall alloy W content; they are higher for the 75 at. % W alloys. The abscissa of Fig. 12b is the W content in the glassy phase that is precursor to the third reaction. For the alloy milled for 20 hr, this W content is the same as that in the as-milled powder (i.e., no crystallization reactions precede the high-temperature one). For alloys milled for 10 hr or less, the abscissa represents the glassy-phase W content following the first reaction. When plotted on this basis, Fig. 12b shows a striking correlation between the temperature of the final crystallization reaction and the glassy-phase composition prior to this reaction.

#### iv - Summary

Our results (coupled with those from ongoing studies) are useful in both a scientific and a technological context. With respect to the latter, we have identified processing conditions and alloy compositions having the greatest potential for consolidation absent crystallization; e.g., a 75 at. % W alloy milled for 20 hr does not crystallize until close to 800° C. This alloy has been chosen as our candidate for future consolidation studies.

Our work is also useful for determining the thermodynamics of the W-Ni system. In particular, measurement of the heat evolved in the various reactions enables changes in phase enthalpies to be determined. From there, it is straightforward to estimate phase free energies. This task will be part of our work for the coming year as is described in Sect. IV. But first we summarize results of our consolidation studies.

### III. Consolidation Studies

Our consolidation studies have proceeded along three routes; hot isostatic pressing (HIP), dynamic compaction, and HIP using a Zr-based metallic glass as a binding agent. We discuss each of these separately.

#### A. Hot Isostatic Pressing (HIP)

---

<sup>2</sup> - Peak temperatures for the second reaction are not shown because the second reaction often overlaps with the third one. This makes a precise measurement of the second reaction temperature difficult.

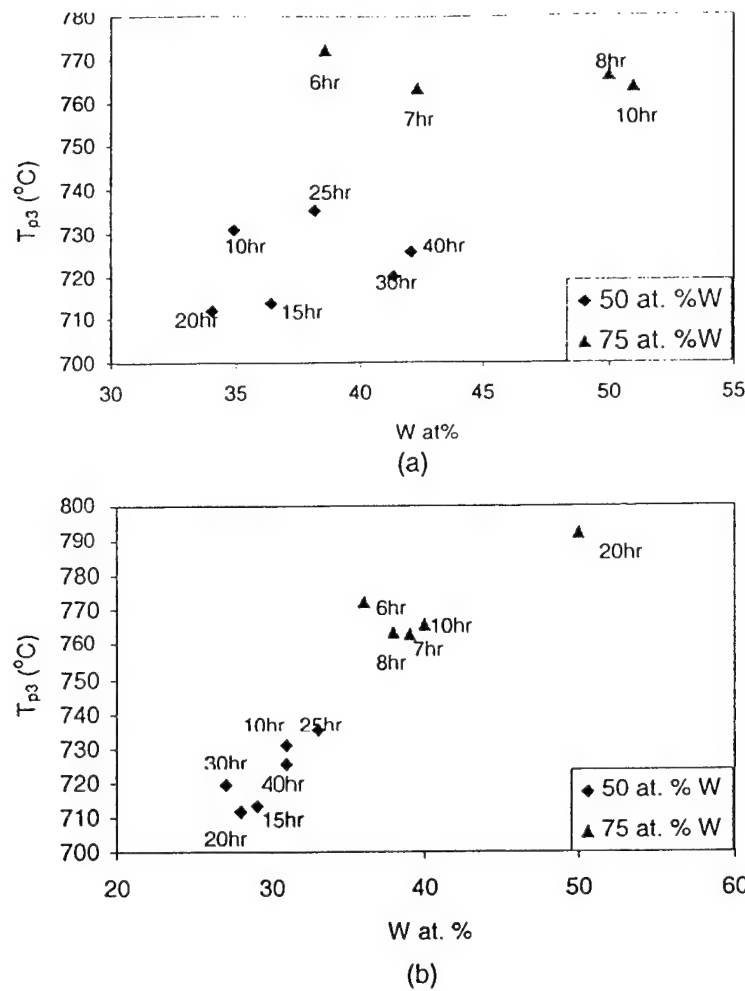


Fig. 12. Peak temperatures for the high-temperature crystallization reaction vs. W content (a) in the glassy phase in the as-milled powders, and (b) in the glassy phase present prior to the high-temperature reaction. (The times shown are milling times.)

We can produce fully dense structures by HIP. However, the temperatures required to do this lead to material crystallization. In retrospect, this is not surprising. That is, material flow (i.e., atomic motion) is needed for densification. But atomic mobility also leads to crystallization. We are no longer pursuing conventional HIP as a consolidation route. However, we mention that the as-consolidated HIP microstructures have a very fine scale (on the order of 100 nm). As such, they display interesting mechanical properties [16].

#### B. Dynamic Compaction

Dynamic compaction experiments were conducted in cooperation with Prof. N. Thadhani of the Georgia Institute of Technology. We supplied Thadhani with as-milled powders. He and his associates dynamically compacted them, and we analyzed the material subsequent to compaction. A report detailing the results of this work has been previously submitted to the Army Research Office. Thus, only the most salient results are presented here.

The material provided to Thadhani was a 75 at.% W alloy having a crystallization temperature of about 780° C. The glassy matrix of this powder contains about 8 vol. % of nanocrystalline W. The Georgia Tech group dynamically compacted three samples having initial powder relative densities of ca. 41, 47, and 52 %. The compacted materials were analyzed at Michigan Tech employing XRD and optical microscopy.

The compacts having the two lesser initial relative densities completely crystallized during compaction. The material with the highest initial relative density only partially crystallized. Moreover, this latter sample was very nearly fully dense. The porosity present was of small size and constituted only several per cent of the material volume. Indeed, some regions of this sample were pore free. However, microcracks were also present, casting some doubt on dynamic compaction's capability for producing flaw-free and fully-dense material. (This is a preliminary assessment.)

Even though dynamically compacted samples were not fully dense, the hardness of their pore-free regions were impressive (Vickers hardness ≈ 13 GPa, corresponding to a yield strength of about 4.5 GPa (≈ 650 ksi)).

#### C. Hot Isostatic Pressing with a "Binding Agent"

Recent work [1] suggests that a Zr-Ti-Ni-Be-Cu metallic glass can "wet" tungsten. Consequently, we have conducted consolidation studies employing powder mixtures of this glass and mechanically alloyed 75 at. % W.

The Zr-base glassy powders were made by first arc-melting the components into a button. Powders were subsequently formed by a hydride-dehydride treatment. Hydriding was accomplished by heat treating the button in flowing hydrogen at 650° C for 3 hr. The button was then "shaken" into powder by placing it in a SPEX mill (without grinding media) for 30 min. The resulting powder was screened to -325 mesh and dehydridization was accomplished by heat treating the powders in vacuum (400° C for 6 hr). A DSC analysis shows that the melting point of the Zr-based glass is 705° C.

Powder mixtures containing 10, 20, 30, and 50 vol. % of the Zr-base glass were prepared. The samples were "quick hipped"<sup>3</sup> at 700-720° C for 20 min at a pressure of 60 ksi. Examination of consolidated materials shows that the W glass does not crystallize during this process. However, the binding agent partially crystallizes. The porosity level of all samples is estimated as less than 7 %. Highest porosity was found in the 10 vol.% Zr-based glass. In distinction, the 50 vol. % Zr-based glass sample is nearly pore free. The results indicate that the Zr-glass does, in fact, function as a binding agent. However, we are surprised that this glass partially crystallizes at a temperature presumably above its melting point.

Microhardnesses of the W-glass microconstituent and the Zr-base glass constituent of consolidated samples were measured. Their hardnesses are comparable - about 4.7 GPa for the W glass and 6.3 GPa for the Zr-glass. While we have not yet achieved a fully dense material by the "quick" HIP process, we plan continuing work along this line because of our promising preliminary results.

#### IV. Future Work

##### A. Thermodynamics of the Ni-W System

There have been prior efforts to characterize the thermodynamics of the Ni-W system. These are based on computational schemes that rely on the phase diagram to provide input data to yield approximate expressions for phase free energies. These are good tools in the absence of thermodynamic property data (such data are sparse). However, they suffer from the problem of extrapolating free energy functions that may be adequate over narrow composition ranges to considerably more extensive composition ranges. For example, estimating the free energy of a glassy phase containing high solute concentrations could be problematic with this approach.

Our DSC studies provide an opportunity to obtain more accurate free energy functions (more precisely, enthalpic functions). We can (and have) measured the energies associated with the various transitions a glassy phase undergoes as it crystallizes. This provides us with differences in phase enthalpies over broad composition ranges. We use one reaction, the low-temperature reaction in 50 at. % W alloys, to illustrate. We know the starting phases (W and the glassy phase) and their compositions (pure W and  $x_{oa}$ ;  $x_{oa}$  varies with milling time). We also know the original phase volume fractions;  $v_{ow}$  (for W) and  $v_{oa}$  (for the glass). And we know the phase volume fractions subsequent to the first reaction (call them  $v_w'$  and  $v_a'$ ) and their compositions (pure W and  $x_a'$ ). We measure the heat evolved ( $\Delta H$ ) during the first reaction;

$$\Delta H = v_a' H_a(x_a') + H_w(v_w' - v_{wo}) - v_{ao} H(x_{ao}) \quad (1)$$

Equations analogous to Eq. (1) can be written for the second and third reactions. We have a number of such  $\Delta H$  values. Moreover, crystalline W is always present as a pure

---

<sup>3</sup> - "Quick" HIP is HIP conducted at a higher pressure and for shorter times than those for conventional HIP.

component, simplifying matters. We also have the enthalpy changes for the fcc-glassy phase transition in pure Ni and the bcc-glassy phase transition in pure W (these are the latent heats of solidification). This further simplifies matters. On the other hand, the compositions of the amorphous phase vary.<sup>4</sup> This complicates matters. However, it is likely that we can develop expressions (e.g., a regular solution model) that mimic this variation of phase enthalpy. We also can estimate solution entropies (usually taken as ideal mixing entropies).

We believe our approach can lead to significantly improved expressions for phase free energies in the Ni-W system.<sup>5</sup> The amount of data we have available is impressive. Success with this problem would lead to designation of more promising compositions to exploit the potential of glassy WHA.

#### B. Consolidation Studies

As mentioned, we plan to continue our quick HIP consolidation work. We may wish to HIP at a somewhat higher temperature than previously in order to achieve full densification. A higher temperature should also preclude partial crystallization of the Zr-base glass. In addition to our studies on the stability of the 75 at. % W glass, we are currently conducting isothermal transformation studies. These will define a "time window" for consolidation absent crystallization.

Following consolidation, mechanical properties (hardness, compressive and tensile flow behavior) will be assessed. The sizes of the samples produced are large enough to permit assessment of tensile flow behavior. To the extent that time and funds permit, we will correlate mechanical properties to deformation and microstructural features of the (W-glass)-(Zr-glass)-crystal composite.

Finally, if funding were available we would consider additional dynamic compaction consolidation in cooperation with Prof. Thadhani. We would have to do sufficient "homework" prior to this to ensure that the temperatures attained during dynamic compaction do not result in crystallization of the W-base glass.

#### V. List of Publications

The publication list below details all publications in the period from February, 1998 to present. Most of these works derived from studies conducted under a prior grant, but did not see print until the period of this grant. However, the topics of both the prior and

---

<sup>4</sup> A complication might arise from coarsening of the nanocrystalline W during the phase transitions. We shall have to compare any heat evolution due to such coarsening to that coming from the phase transformations. Ordinarily a "heat of coarsening" is quite small compared to a heat of reaction. However, this might not be the situation with nanocrystalline particles. The matter is capable of being addressed, though.

<sup>5</sup> - Some approximations are employed in our treatment. The most obvious is our assumption that Fe and Ni chemically behave the same in our systems. They do not, of course. But as noted earlier they do behave quite similarly.

currently expiring grant were similar in that they dealt with various aspects of mechanical alloying process.

S. Mi and T. H. Courtney, "Processing, Structure, and Properties of Ni-W Alloys Fabricated by Mechanical Alloying and Hot-Isostatic Pressing," *Scripta Mater.*, vol. 38, p. 637, (1998).

B. R. Murphy and T. H. Courtney, "Mechanochemically Synthesized NbC Cermets: Part I – Synthesis and Structural Development," *J. Mater. Res.*, vol. 14, p. 4274, (1999).

B. R. Murphy and T. H. Courtney, "Mechanochemically Synthesized NbC Cermets: Part II – Mechanical Properties," *J. Mater. Res.*, vol. 14, p. 4285, (1999).

A. N. Streletskeii and T. H. Courtney, "Kinetic, Chemical, and Mechanical Factors Affecting Mechanical Alloying of Ni-BCC Transition Metal Mixtures," *Mat. Sc. And Eng.*, A282, p. 213, (2000).

Z. He and T. H. Courtney, "Crystallization and Thermal Stability of Mechanically Alloyed W-Ni-Fe Noncrystalline Materials," submitted for publication.

#### VI. Scientific Personnel Supported

Professor Courtney was supported one summer month during 1998. Mr. Zhi He has been supported by this grant for its duration. He is a Ph.D. student whose completion date is anticipated as Spring, 2001.

Dr. A. N. Streletskeii of the N.N. Semenov Institute of Chemical Physics, Russian Academy of Sciences, Moscow was a guest of Prof. Courtney during a portion of 1998. Streletskeii received no support from this grant (he was supported by the COBASE program of the National Academy of Sciences), but the area in which he and Courtney collaborated was related to the overall thrust of this program. As noted in the previous section, a paper resulted from this collaborative effort.

#### VII. References

1. R. D. Conner and W. L. Johnson, *Acta Mater.*, 46, (1998), 6089.
2. Y. H. Kim, K. Hiraga, A. Inoue and T. Masumoto, *Mater. Trans. JIM*, 35, (1994), 293.
3. C. Fan and A. Inoue, *Mater. Trans. JIM*, 38, (1997), 1040.
4. A. Inoue, T. Zhang and Y. H. Kim, *Mater. Trans. JIM*, 38, (1997), 749.
5. J. Eckert, A. Kubler and L. Schultz, *J. Appl. Phys.*, 85, (1999), 7112.
6. Y. Leng and T. H. Courtney, *Metall. Trans. A*, 21A, (1990), 2159.
7. Y. Leng and T. H. Courtney, *J. Mater. Sc.*, 24, (1989), 2006.
8. Y. Leng and T. H. Courtney, *J. Mater. Sc.*, 26, (1991), 588.
9. A. O. Aning, Z. Wang and T. H. Courtney, *Acta Metall. Mater.*, 41, (1993), 165.
10. Z. He and T. H. Courtney, submitted for publication.
11. T. H. Courtney and Z. Wang, *Scr. Metall. Mater.*, 27, (1992), 777.
12. C. G. Mukira, Ph.D. Thesis, Michigan Technological University, (1997).

13. B. D. Cullity, Elements of X-Ray Diffraction, Addison-Wesley, Reading, MA, (1977), p. 415.
14. P. Nash, Ed., Phase Diagrams of Binary Nickel Alloys, ASM International, Materials Park, OH, (1991), p. 369.
15. E. Epremian and D. Harker, Trans. AIME, 185, (1949), 267.
- 16.C. G. Mukira and T. H. Courtney, Proc. 2<sup>nd</sup> Intl. Conf. On Tungsten and Refractory Metals, A. Bose and R. J. Dowding, Ed., Metal Powder Industries Federation, Princeton, NJ, (1994), p. 157.